

# Cardiac Sarcoidosis: The Role of Multimodal Imaging

Lara Cristiane Terra Ferreira Carreira,<sup>1</sup> Livia Carreira,<sup>2</sup> Adriana Soares Xavier de Brito<sup>3,4</sup>

Cardiologia Nuclear de Curitiba (CNC),<sup>1</sup> Curitiba, PR – Brazil

PUC Paraná,<sup>2</sup> Curitiba, PR – Brazil

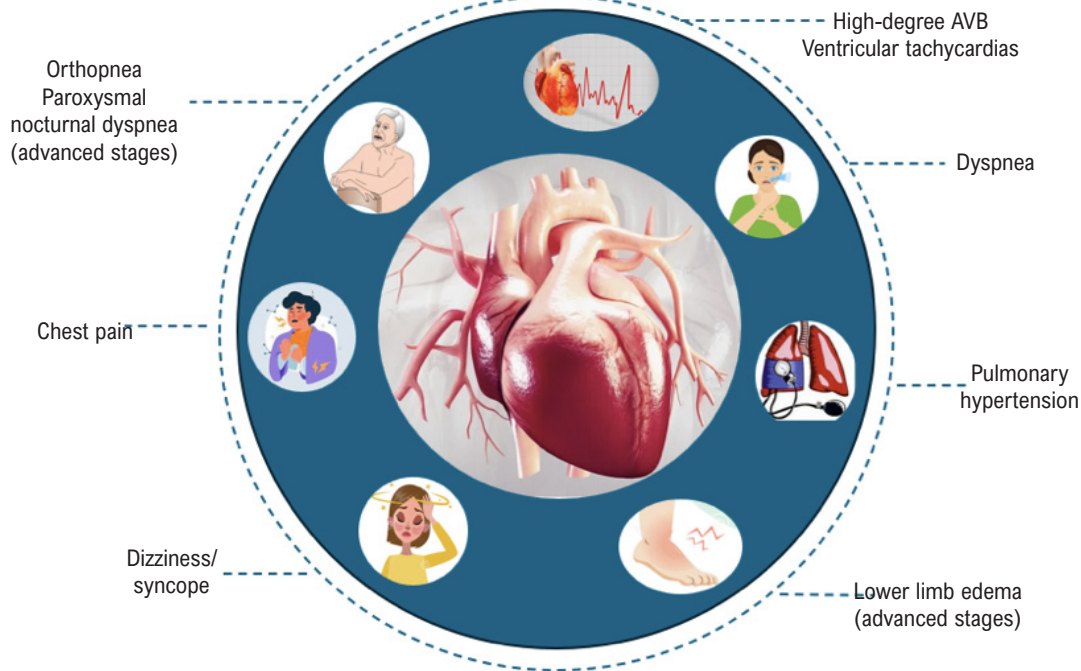
Instituto Nacional de Cardiologia,<sup>3</sup> Rio de Janeiro, RJ – Brazil

Rede D’Or São Luiz,<sup>4</sup> Rio de Janeiro, RJ – Brazil

Central Illustration: Cardiac Sarcoidosis: The Role of Multimodal Imaging



## Cardiac sarcoidosis



Arq Bras Cardiol: Imagem cardiovasc. 2026; 39(1):e20250038

Central Illustration: Clinical manifestations of cardiac sarcoidosis. AVB: atrioventricular block.

### Keywords

Sarcoidosis; Positron-Emission Tomography; Fluorodeoxyglucose F18; Magnetic Resonance Imaging; Multimodal Imaging.

Mailing Address: Adriana Soares Xavier de Brito •

Instituto Nacional de Cardiologia. Rua das Laranjeiras, 374. Postal code: 22240-006. Rio de Janeiro, RJ – Brazil

E-mail: adrijssoares@hotmail.com

Manuscript received February 8, 2026; revised February 9, 2026; accepted February 9, 2026

Editor responsible for the review: Marcelo Tavares

DOI: <https://doi.org/10.36660/abcimg.20250038>

### Abstract

Cardiac sarcoidosis (CS) is a potentially severe manifestation of systemic sarcoidosis, associated with advanced atrioventricular block, ventricular arrhythmias, heart failure, and sudden death. Diagnosis remains challenging due to phenotypic variability and the limitations of conventional diagnostic methods. Advances in imaging techniques, especially the combination of positron emission tomography/computed tomography (PET/CT) using <sup>18</sup>F-FDG and cardiac magnetic resonance imaging (CMR), have revolutionized the diagnostic

approach and therapeutic monitoring of CS. This article reviews current concepts of CS and its diagnosis, with a focus on the role of PET/CT, the importance of appropriate patient preparation, and integration with CMR.

## Introduction

Sarcoidosis is an inflammatory granulomatous disease of unknown etiology, characterized by non-caseating granulomas that can affect multiple organs.<sup>1,2</sup>

The disease affects the lungs and thoracic lymph nodes in approximately 90% of cases, but it can also involve the heart, liver, spleen, skin, eyes, parotid glands, among other organs and tissues. It is estimated that 20% to 25% of patients with pulmonary and/or systemic sarcoidosis have asymptomatic cardiac involvement (clinically silent disease),<sup>2</sup> whereas approximately 5% have clinically manifest cardiac involvement. This involvement is associated with increased morbidity and mortality, resulting from infiltrative heart disease with intense myocardial inflammation.

Approximately half of cardiac sarcoidosis (CS) cases occur in isolation, without evidence of systemic sarcoidosis.<sup>1</sup>

The pathophysiology of CS involves an exaggerated immune response to environmental antigens in individuals who are genetically predisposed. This response culminates in the activation of T cells and the formation of granulomas, with subsequent progression to myocardial fibrosis. The disease most frequently affects individuals between 25 and 55 years of age, with higher prevalence among women, Black individuals, and Japanese populations. It is also responsible for a significant proportion of sudden death in young adults.<sup>3</sup>

CS can manifest as arrhythmias, atrioventricular blocks, dilated cardiomyopathy, or sudden death. Cardiac symptoms are usually dominant, as patients often present only with low-grade pulmonary involvement and no other organ involvement.<sup>2</sup> The high morbidity and mortality make early and accurate diagnosis essential (Central Illustration).

The prevalence of CS has increased during the last two decades, probably due to the use of advanced cardiac imaging. At the same time, it remains a reversible cause of cardiomyopathy and arrhythmias that is frequently underdiagnosed.

## Clinical diagnosis and current criteria

Investigation for CS should be performed in individuals with known systemic sarcoidosis, especially when other organs are involved. In addition, CS should be suspected in patients under 55 years of age who present with atrioventricular block (AVB), ventricular arrhythmias, or heart failure of unclear etiology.

Diagnosis of CS remains challenging due to the limited sensitivity and specificity of any single diagnostic modality, highlighting the importance of high clinical suspicion, the use of multimodal imaging to guide diagnosis and

treatment, and histological findings.

Endomyocardial biopsy remains the gold standard for CS diagnosis, but, due to the irregular and predominantly mesocardial pattern of involvement, it has a diagnostic yield of around 25% to 30%, with a high rate of false negatives. There is, therefore, an ongoing debate regarding the real need for histological confirmation for definitive diagnosis.<sup>4</sup>

The main diagnostic criteria for CS have been established by the Heart Rhythm Society (HRS)<sup>5</sup> and the Japanese Circulation Society (JCS).<sup>6</sup> According to the HRS, definitive diagnosis requires histological confirmation of non-caseating granulomas in the myocardium, whereas probable diagnosis can be established in the presence of confirmed extracardiac sarcoidosis and typical evidence of cardiac involvement, either by imaging or characteristic clinical manifestations. On the other hand, the JCS admits the diagnosis of isolated CS even in the absence of histological confirmation, provided that there are compatible clinical and imaging findings, allowing greater sensitivity in detecting cases without apparent systemic sarcoidosis.

Even though these criteria are still widely used, especially in regional contexts, no set of criteria is perfect or universally applicable.

The current trend is to abandon the rigid and binary use of these criteria (positive/negative) and adopt an integrated probabilistic approach, classifying the diagnosis as:

- Definite
- Highly probable
- Probable
- Possible/low probability

This approach is inspired by the World Association of Sarcoidosis and Other Granulomatous Disorders (WASOG) classification and has been adopted by multiple authors to incorporate the relative weight of clinical, laboratory, and advanced imaging findings (CMR and PET, Figure 1) in the final probability of CS.<sup>3</sup>

Sarcoidosis is often called “the great mimicker,” due to its diverse manifestations and must be differentiated from other cardiac syndromes with a similar phenotype, such as acute myocarditis, chronic inflammatory cardiomyopathies (including those related to autoimmune, hereditary and infiltrative diseases) and other granulomatous diseases. Clinical context and cardiac imaging are often insufficient to differentiate sarcoidosis from other forms of cardiac pathology that cause hereditary arrhythmogenic cardiomyopathies or myocarditis. The wide spectrum of clinical presentations and the limitations in obtaining histopathological confirmation, especially in cases of clinically isolated CS, are additional challenges in distinguishing it from alternative diagnoses. To address this complexity, a multidisciplinary team is needed, composed of specialists in systemic sarcoidosis, heart failure, electrophysiology, advanced cardiac imaging, cardiovascular genetics, and cardiac pathology.<sup>3</sup>

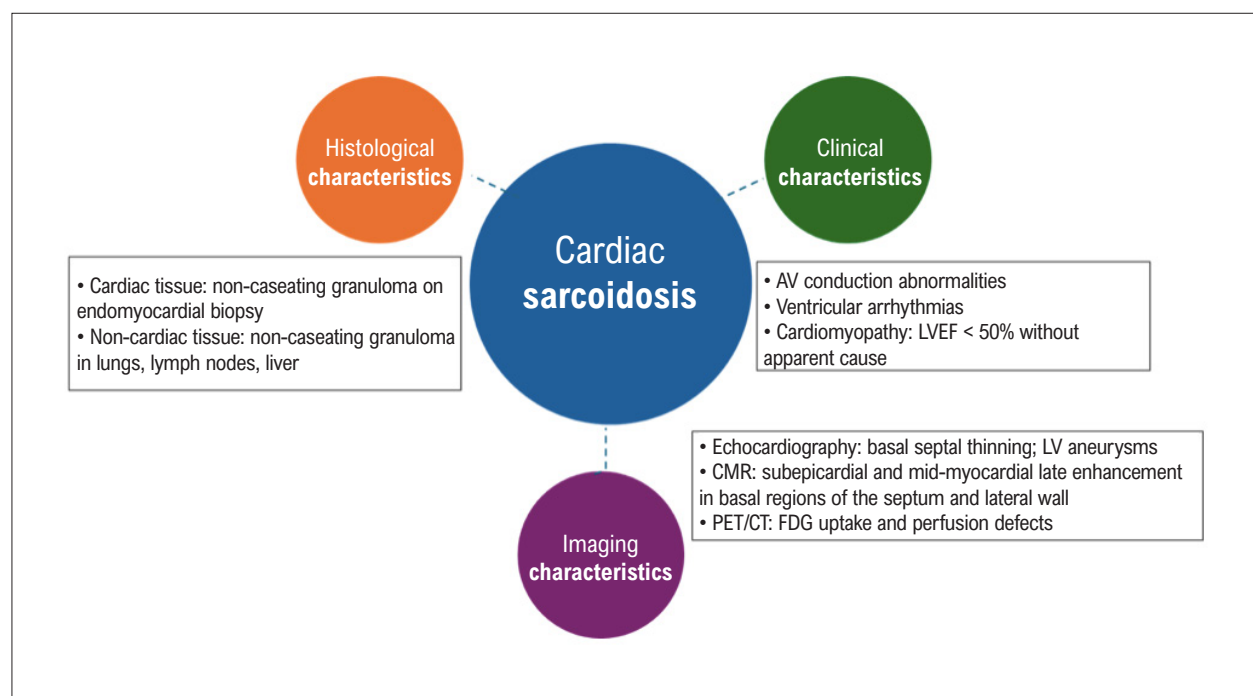


**Figure 1** – Diagnosis of cardiac sarcoidosis. AV: atrioventricular; CMR: cardiac magnetic resonance imaging; FDG: fluorodeoxyglucose; LV: left ventricle; LVEF: left ventricular ejection fraction; PET/CT: positron emission tomography/computed tomography.

## Diagnostic modalities

### Electrocardiography

Although widely available, electrocardiography (ECG) has limited sensitivity and specificity for the diagnosis of CS.<sup>7</sup> Nevertheless, diagnostic guidelines have incorporated some ECG abnormalities as criteria, including conduction disturbances, AVB, frequent or multifocal ventricular extrasystoles, right or left bundle branch blocks, and abnormal Q waves.<sup>5,6</sup>

Holter ECG can increase suspicion for CS in the presence of frequent ventricular extrasystoles, high-grade conduction abnormalities, or ventricular arrhythmias such as ventricular tachycardia.<sup>3</sup>

### Echocardiography

Transthoracic echocardiography is widely available and can be used as an initial tool to detect structural and functional abnormalities in the heart, although it does not provide detailed tissue characterization.<sup>7</sup> Although abnormal echocardiography is useful for determining cardiac involvement in patients with suspected CS (low to moderate sensitivity), a normal echocardiogram does not rule out the presence of cardiac involvement (low specificity). Abnormal findings that support diagnosis of CS include septal thinning, abnormal ventricular wall anatomy (ventricular aneurysm or regional ventricular wall thickening), unexplained left ventricular (LV) systolic dysfunction, or LV dilation.<sup>8</sup> When combined with clinical

symptoms, ECG or Holter abnormalities, echocardiography increases the sensitivity for detecting CS. Furthermore, more recent echocardiographic approaches, including global longitudinal strain measurements, can assist in accurately identifying patients with CS who have preserved left ventricular ejection fraction (LVEF).<sup>9</sup>

Despite its limited sensitivity and specificity, echocardiography remains useful for initial screening and serial monitoring of CS due to its wide availability and low cost.

### Myocardial perfusion imaging

Myocardial perfusion scintigraphy generally shows segmental areas of reduced tracer uptake in the ventricular myocardium of patients with CS, making it useful in resting assessment of scars resulting from microvascular compression and/or fibrogranulomatous replacement of myocardial tissue, which can generate perfusion defects. Generally, these defects do not follow the typical vascular distribution pattern of coronary artery disease, except in cases of very extensive involvement. Therefore, they are nonspecific findings and can be observed in ischemic dilated cardiomyopathies or cardiomyopathies of other etiologies. Thus, myocardial perfusion imaging alone is not sufficient to confidently establish the diagnosis of CS, especially in the absence of cardiac symptoms.

On the other hand, positron emission tomography/computed tomography (PET/CT) using <sup>18</sup>F-fluorodeoxyglucose (<sup>18</sup>F-FDG) for assessment of myocardial metabolism, associated with perfusion imaging

performed with  $^{13}\text{N}$ -ammonia,  $^{82}\text{Rb}$  or, alternatively, single-photon emission computed tomography (SPECT) using  $^{99\text{m}}\text{Tc}$ -sestamibi, has emerged as a valuable tool in the diagnosis and staging of CS. This hybrid approach allows simultaneous identification of active inflammation and areas of fibrosis, contributing to improved stratification of disease activity and chronicity.<sup>10</sup>

### Cardiac magnetic resonance imaging

Cardiac magnetic resonance imaging (CMR) is a high-spatial-resolution modality that, in addition to providing detailed assessment of biventricular function, identifies and quantifies areas of myocardial injury, including edema and fibrosis, primarily through late gadolinium enhancement (LGE).

Gadolinium is an extracellular contrast agent with rapid elimination from normal myocardium, but slow elimination from areas of fibrosis and inflammation, resulting in delayed enhancement in expanded extracellular space.

CMR allows for precise, non-invasive evaluation of the entire heart with high accuracy in detecting focal myocardial changes typical of CS, in both the acute (edema) and chronic (fibrosis) phases. Furthermore, it provides detailed information on cardiac structure and function, also enabling the identification of mediastinal and hilar lymphadenopathy, hepatosplenic changes, and pulmonary nodules that may suggest extracardiac sarcoidosis. The technique is also capable of detecting other cardiomyopathies and ischemic disease, which reinforces its value in differential diagnosis.

CMR has become a fundamental tool in the diagnostic assessment of CS, and it is routinely recommended in patients with clinical suspicion of the disease, especially given the well-recognized limited sensitivity of echocardiography.<sup>10</sup>

Using clinical criteria as a reference standard and non-ischemic LGE patterns as a definition of positivity, CMR demonstrated high sensitivity (95%) and specificity (85%) for diagnosis of CS, according to a meta-analysis of 17 studies involving 1,031 individuals.<sup>11</sup>

The presence of LGE is the strongest predictor of all-cause mortality and sustained ventricular arrhythmias in individuals with known or suspected CS.<sup>12</sup>

A systematic review and meta-analysis of macroscopic pathological images of hearts with histologically confirmed CS identified common sites of myocardial involvement. LV subepicardial, interventricular septum, LV multifocal, and right ventricular free wall involvement were observed in more than 90% of cases (frequent pathological features).<sup>13</sup>

In many cases, however, the LGE pattern may be nonspecific, making it difficult to differentiate between CS, myocarditis, and other cardiomyopathies. Therefore, no single LGE pattern is sufficient to establish the diagnosis of CS. It is thus recommended that CMR findings be analyzed by a multidisciplinary team within a multimodal framework.

CMR also provides a high negative predictive value, both to rule out the disease and to identify patients with a low event rate, and it may be useful in assessing

other differential diagnoses (e.g., arrhythmogenic right ventricular cardiomyopathy, myocarditis, prior myocardial infarction).

### Positron emission tomography/computed tomography using $^{18}\text{F}$ -fluorodeoxyglucose

FDG, a glucose analogue, is sequestered in activated inflammatory cells, such as macrophages and lymphocytes, via insulin-independent glucose transporter proteins (GLUT1 and GLUT3) and, therefore, accumulates in areas of regulated glucose metabolism, including hypermetabolic sites of myocardial sarcoid infiltration. Thus, it detects metabolically active inflammatory lesions.

Reviews have reported a diagnostic sensitivity of 91% and specificity of 75.5% for  $^{18}\text{F}$ -FDG-PET/CT in the diagnosis of CS. The main cause of the limited specificity and high variability seems to be associated with physiological FDG uptake in normal myocardium. Therefore, adequate preparation for the study is essential to accurately diagnose CS using  $^{18}\text{F}$ -FDG-PET/CT.

Cardiac  $^{18}\text{F}$ -FDG-PET/CT provides useful anatomical and morphological information to assess the location, extent, activity, and stage of the disease. As a complementary modality to CMR, it enables non-invasive image-guided diagnosis and identifies extracardiac sites suitable for biopsy, contributing to histological confirmation of systemic sarcoidosis.

Furthermore, it is applied for monitoring therapeutic response, longitudinal follow-up, risk stratification, and prognosis.<sup>14</sup>

The most characteristic pattern of CS on  $^{18}\text{F}$ -FDG-PET/CT is multifocal radiopharmaceutical uptake, particularly when associated with resting perfusion defects (metabolic-perfusion mismatch pattern), reflecting disruption between perfusion and metabolism (Figure 2B). In some cases, focal FDG uptake restricted to the interventricular septum (even in the absence of late enhancement on CMR) may be the only imaging sign of sarcoid involvement, especially in patients with heart block (Figure 2A). When active inflammatory tissue is replaced by fibrosis, FDG uptake is not observed at the LGE sites (match pattern), i.e., metabolically inactive disease (Figure 2C). Findings of FDG uptake that can lead to false positives result from inadequate physiological suppression or increased glucose uptake in conditions such as hibernating myocardium, inflammatory or genetic dilated cardiomyopathies, recent infarction, and inflammatory responses following recent cardiac procedures such as ventricular ablation (Figure 2D).<sup>3</sup>

The extent of FDG uptake has been correlated with the risk of adverse events such as death, ventricular arrhythmias, and hospitalizations for heart failure, although CMR with LGE has shown superior prognostic capacity in some studies.<sup>15</sup>

Although there is still not enough data to justify the exclusive use of FDG-PET for risk stratification of sudden cardiac death, its association with CMR and clinical data may be valuable for prognostic assessment.

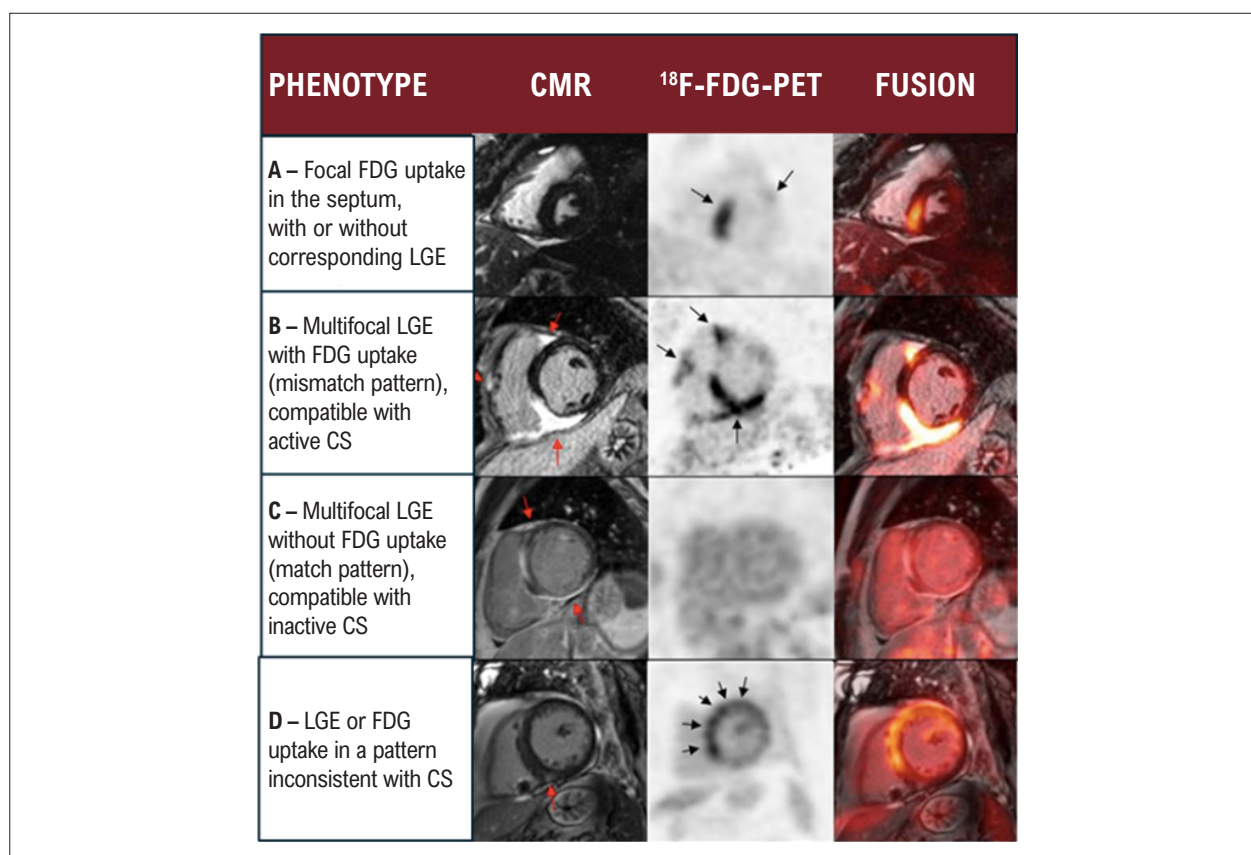


**Figure 2** – Findings on cardiac magnetic resonance and <sup>18</sup>F-FDG-PET according to disease phenotype (adapted from Cheng et al.3). CMR: cardiac magnetic resonance imaging; CS: cardiac sarcoidosis; FDG: fluorodeoxyglucose; LGE: late gadolinium enhancement; PET: positron emission tomography.

### Patient preparation for <sup>18</sup>F-FDG-PET with: suppression of physiological FDG uptake in normal myocardium

It is important to emphasize that glucose is a common energy source in healthy myocardial cells; however, unlike inflammatory cells, cardiomyocytes absorb glucose via an insulin-dependent mechanism (GLUT4) regulated by fasting and dietary composition. During fasting, more than 90% of myocardial energy metabolism is derived from fatty acid metabolism. Most of the remaining 10% involves other substances, including glucose. However, myocardial glucose metabolism during fasting varies among individuals, and in some cases, FDG uptake is observed in the myocardium even under fasting conditions. This variability can compromise <sup>18</sup>F-FDG-PET images of myocardial inflammation and affect diagnostic accuracy. Consequently, inducing a metabolic shift in the heart, defined as the transition from glucose utilization to fatty acids and fatty acid-derived ketones, can lead to the suppression of normal FDG uptake in the heart (through inhibition of GLUT4 translocation) and the identification of FDG-avid inflammatory cells.

The goal is to suppress physiological uptake of glucose by the myocardium. To this end, a high-fat, low-carbohydrate diet is recommended for 12 to 24 hours, followed by prolonged fasting for 12 to 18 hours before the examination. Intravenous

administration of unfractionated heparin (50 IU/kg), 15 minutes before FDG injection, has also been considered and performed by some centers. Physical activity should be avoided for 24 hours before the examination (at least 12 hours), as it increases myocardial FDG uptake. Adequate sleep the night before the examination is also recommended (Figure 3).

In the case of insulin-dependent patients with diabetes, insulin use is not permitted on the day of the examination. Serum glucose level must be below 180 mg/dL.<sup>16</sup>

Images are acquired approximately 60 to 90 minutes after FDG injection.

### Interpretation of cardiac <sup>18</sup>F-FDG-PET/CT

Interpretation of <sup>18</sup>F-FDG-PET/CT images in CS is based on the identification of FDG uptake patterns, such as focal or focal-over-diffuse uptake, which are indicative of active inflammation.

Semiquantitative analysis, using the standardized uptake value (SUV), can help quantify inflammatory activity and assess treatment response,<sup>17</sup> although there is no evidence relating specific SUV values to clinical outcomes, nor is there a validated SUV threshold that differentiates CS from normal myocardium.

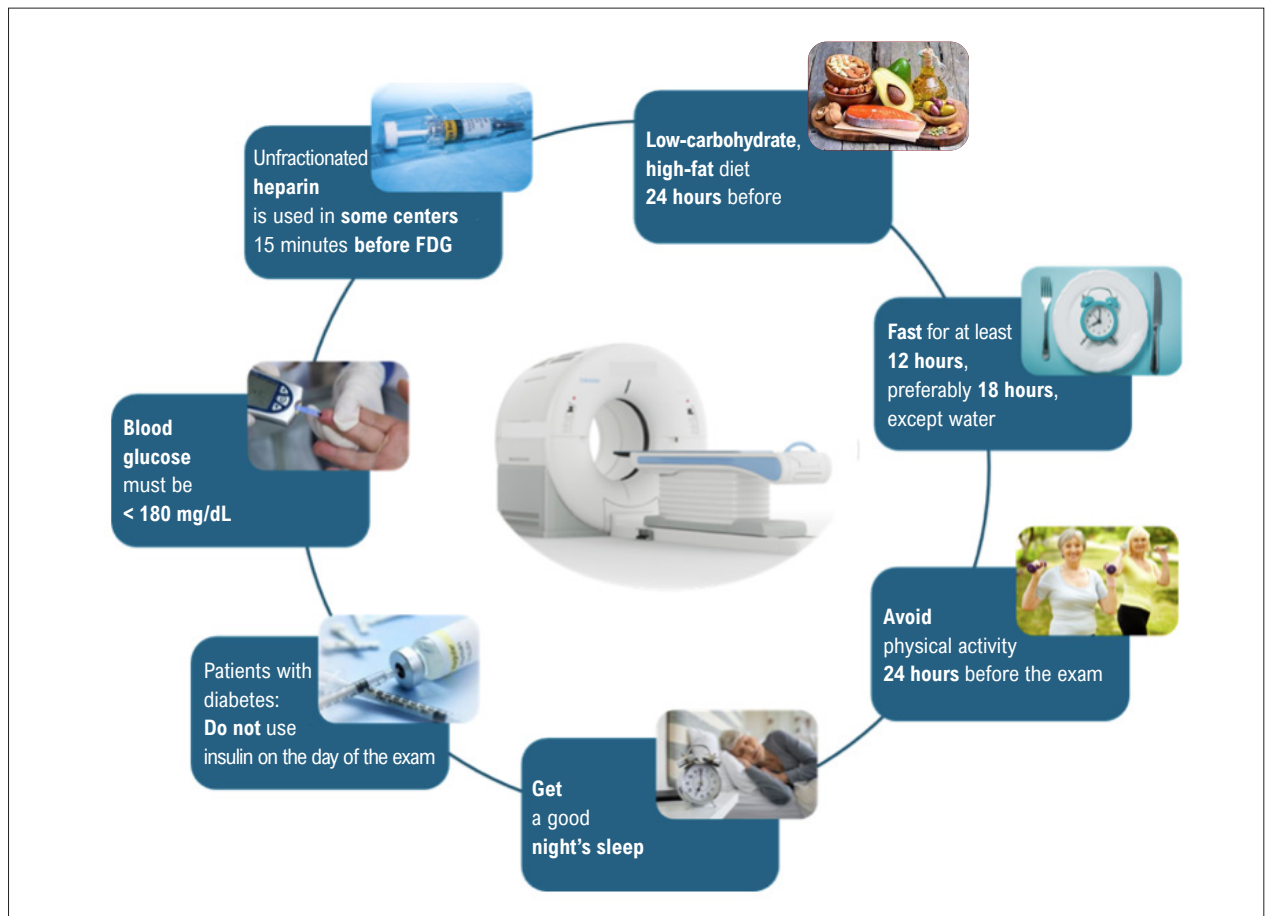


**Figure 3** – Patient preparation for  $^{18}\text{F}$ -FDG-PET/CT. FDG: fluorodeoxyglucose; PET/CT: positron emission tomography/computed tomography.

In the context of monitoring treatment response, FDG-PET is used to assess changes in inflammatory activity after the introduction of immunosuppressive therapies, such as corticosteroids. A reduction in FDG uptake after treatment is associated with a favorable response.<sup>17</sup>

### Combined analysis of CMR and FDG-PET

Studies have demonstrated that the hybrid CMR/FDG-PET approach improves diagnostic and prognostic accuracy in patients with CS. The simultaneous presence of LGE and FDG uptake is a strong indicator of active CS, associated with an increased risk of adverse cardiac events, such as cardiac arrest and ventricular tachycardia.<sup>18</sup>

Furthermore, the combination of these modalities enhances risk stratification and monitoring of treatment response, especially in patients with suspected or confirmed cardiac involvement.<sup>19</sup>

The hybrid approach is also useful in complex cases, for example, patients with prior myocardial infarction, where differentiating between post-infarction fibrosis and sarcoid inflammation may be challenging.

Therefore, the combination of FDG-PET and CMR provides a more comprehensive view of cardiac pathology, supporting clinical decision-making and therapeutic management of CS.

### Final considerations

In patients with clinical suspicion of sarcoidosis with cardiac involvement, CMR represents an excellent screening modality, as the absence of LGE is associated with a high negative predictive value, as well as excellent prognosis. In patients with contraindications to CMR and symptoms suggestive of active disease, FDG-PET combined with resting myocardial perfusion scintigraphy can also be used for the diagnosis of cardiac and extracardiac disease. In addition, serial assessment of inflammation using FDG-PET has been recommended to monitor response to therapy, thus guiding the duration and choice of medications. Despite growing recognition that CMR and FDG-PET imaging can identify patients at higher risk of adverse events, randomized multicenter trials are lacking to guide and standardize follow-up. Future studies are needed to determine the benefits of image-guided therapies, with the aim of improving these patients' prognosis.

### Illustrative clinical cases

**Case 1** – A 68-year-old female patient with hypertension presented to the emergency department due to tachycardia and dyspnea at rest. ECG revealed sustained ventricular tachyarrhythmia and clinical signs of decompensated heart failure. Immediate electrical cardioversion was performed, and intravenous amiodarone was administered. Invasive coronary angiography revealed nonobstructive coronary arteries, severe LV systolic dysfunction, and diffuse hypokinesia. CMR revealed moderate left atrial enlargement, LV with global systolic dysfunction (LVEF = 40%). A moderate amount of multifocal LGE was present, unrelated to coronary topography. Enhancement was transmural in the anterior segments (apical and basal); heterogeneous and mid-myocardial to subepicardial in the inferior and anterolateral (medial and basal) segments, with endocardial sparing; and heterogeneous along the right ventricular side of the interventricular septum. The pattern was thus compatible with CS (Figure 4A). Pulse therapy with intravenous corticosteroids was indicated, followed by implantation of a cardioverter-defibrillator.

Two months after hospital discharge, with reduced dose of corticosteroids, the patient presented with fatigue on exertion, palpitations, and afternoon fever. There were no other symptoms of infection, and leukogram revealed mild leukocytosis. Recurrence of myocardial inflammation due to active disease was suspected. PET/CT with  $^{18}\text{F}$ -FDG associated with resting myocardial perfusion scintigraphy with  $^{99\text{m}}\text{Tc}$ -sestamibi was requested to assess inflammation

and perfusion. Scintigraphy demonstrated anteroseptal, septoapical, and apical hypoperfusion, LVEF of 29%, diffuse hypokinesia, and akinesia of the apical segments (Figure 4B).  $^{18}\text{F}$ -FDG-PET/CT revealed abnormal radiopharmaceutical uptake throughout the anterior and septal walls of the LV, sparing the inferolateral wall, corresponding to an active inflammatory process, with a pattern described as “focal-on-diffuse” (Figure 4C).

Prednisone was resumed at a dose of 1 mg/kg/day, and methotrexate was added to the treatment. She showed a good response and significant clinical improvement

**Case 2** – A 56-year-old male patient without comorbidities received a diagnosis of myocardial infarction with non-obstructive coronary arteries (MINOCA) after hospital admission for chest pain and dyspnea, with coronary computed tomography angiography and invasive coronary angiography showing no obstructive lesions. CMR demonstrated increased LV volumes, reduced wall thickness, and akinesia of the inferior, inferoseptal, and basal inferolateral segments. The myocardial mass with LGE was estimated at 27% of the LV. Echocardiography confirmed these findings, with akinesia and thinning of the basal segment of the inferior wall, hypokinesia of the remaining walls, more pronounced in the inferior and inferolateral septum, and global LV dysfunction (LVEF = 35%). ECG showed sinus rhythm, first degree AVB, and complete left bundle branch block. He remained on clinical treatment for heart failure and MINOCA.

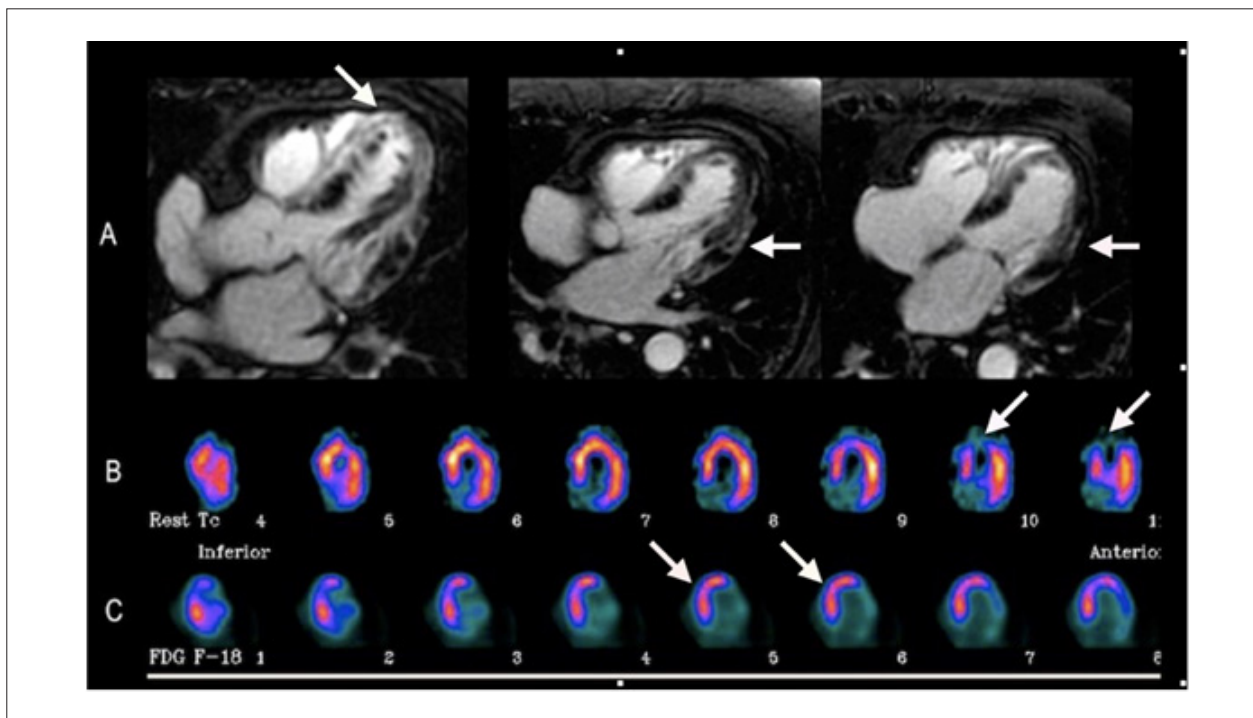


**Figure 4** – (A) Cardiac magnetic resonance imaging with gadolinium demonstrating late enhancement in the septo-apical and lateral regions. (B) Myocardial perfusion scintigraphy with  $^{99\text{m}}\text{Tc}$ -sestamibi – horizontal long axis demonstrating hypoperfusion in the apical segments. (C)  $^{18}\text{F}$ -FDG PET/CT with abnormal radiotracer uptake in the left ventricle, sparing the inferolateral wall, representing a focal-on-diffuse pattern. FDG: fluorodeoxyglucose; PET/CT: positron emission tomography/computed tomography.

Two years later, the patient's functional class worsened, with progressive fatigue during even moderate exertion. A 24-hour Holter ECG demonstrated periods of complete AVB, and the patient was referred for pacemaker implantation, with suspected inflammatory/infiltrative disease. He was also referred for PET/CT with  $^{18}\text{F}$ -FDG and resting myocardial perfusion scintigraphy with  $^{99\text{m}}\text{Tc}$ -sestamibi to assess inflammation and perfusion.

SPECT/CT scintigraphy demonstrated pronounced hypoperfusion throughout the inferior, inferolateral, and basal inferoseptal walls, LVEF of 31%, diffuse hypokinesia and akinesia of the inferior wall, and inferoseptal dyskinesia (Figures 5 and 6, respectively). An  $^{18}\text{F}$ -FDG-PET/CT scan revealed abnormal uptake of the radiopharmaceutical in the septal region, inferior region, and throughout the lateral wall, corresponding to an active inflammatory process (Figure 7), demonstrating a metabolic-perfusion mismatch, a pattern described as focal-on-diffuse. In addition, there was increased uptake in subcarinal lymph nodes and pulmonary hila. Lymph node biopsy confirmed the diagnosis of sarcoidosis, and the patient underwent corticosteroid therapy, with a favorable response in terms of functional class and improved LV function.

## Author Contributions

Conception and design of the research, acquisition of data, analysis and interpretation of the data, writing of the manuscript and critical revision of the manuscript for intellectual content: Carreira LCTF, Carreira L, Brito ASX.

## Potential Conflict of Interest

No potential conflict of interest relevant to this article was reported.

## Sources of Funding

There were no external funding sources for this study.

## Study Association

This study is not associated with any thesis or dissertation work.

## Ethics Approval and Consent to Participate

This article does not contain any studies with human participants or animals performed by any of the authors.

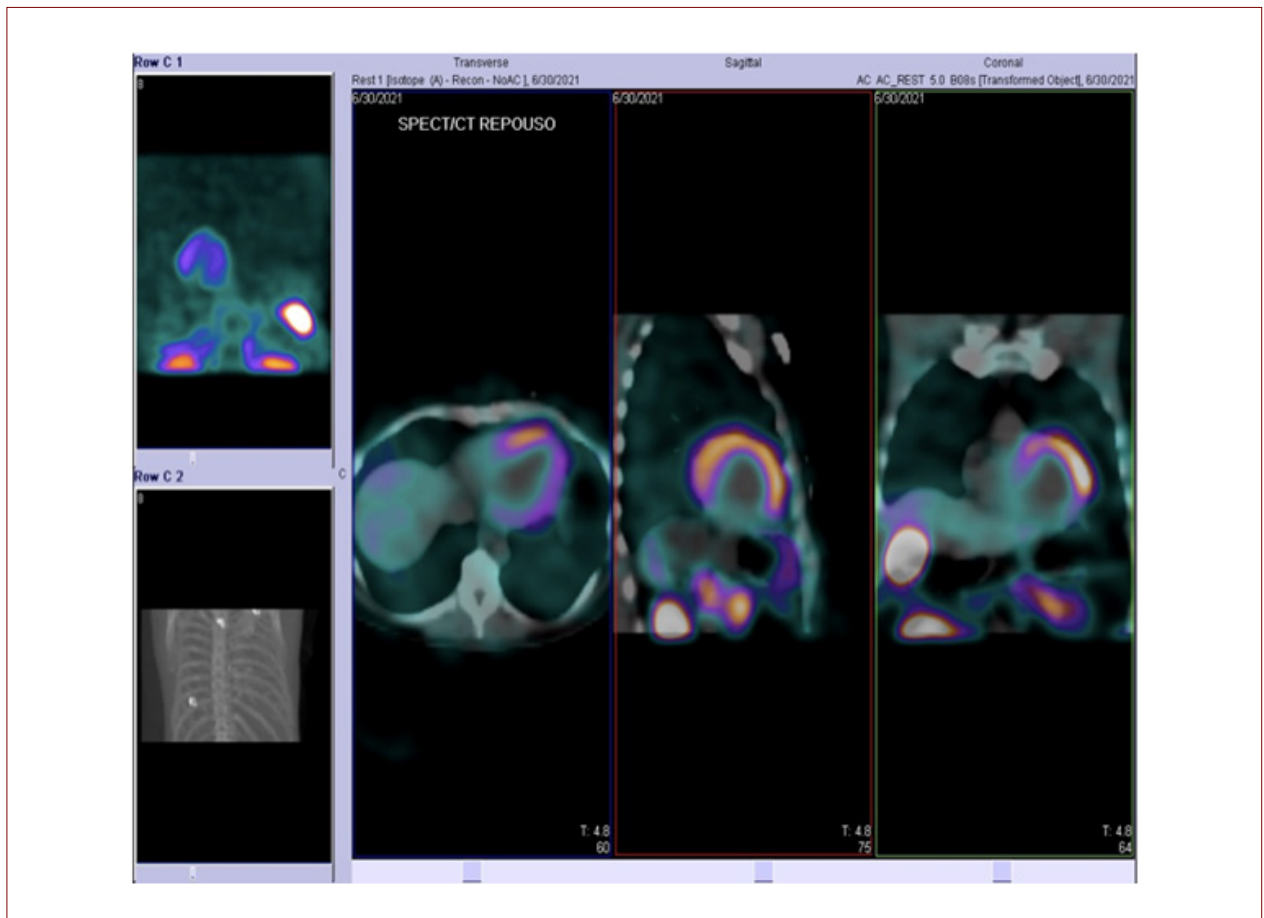


**Figure 5** – SPECT/CT with  $^{99\text{m}}\text{Tc}$ -sestamibi showing fusion images in the axial, sagittal, and coronal axes demonstrating pronounced hypoperfusion of the radiotracer in the inferior, inferoseptal, and inferolateral walls of the left ventricle. SPECT/CT: single-photon emission computed tomography/computed tomography.

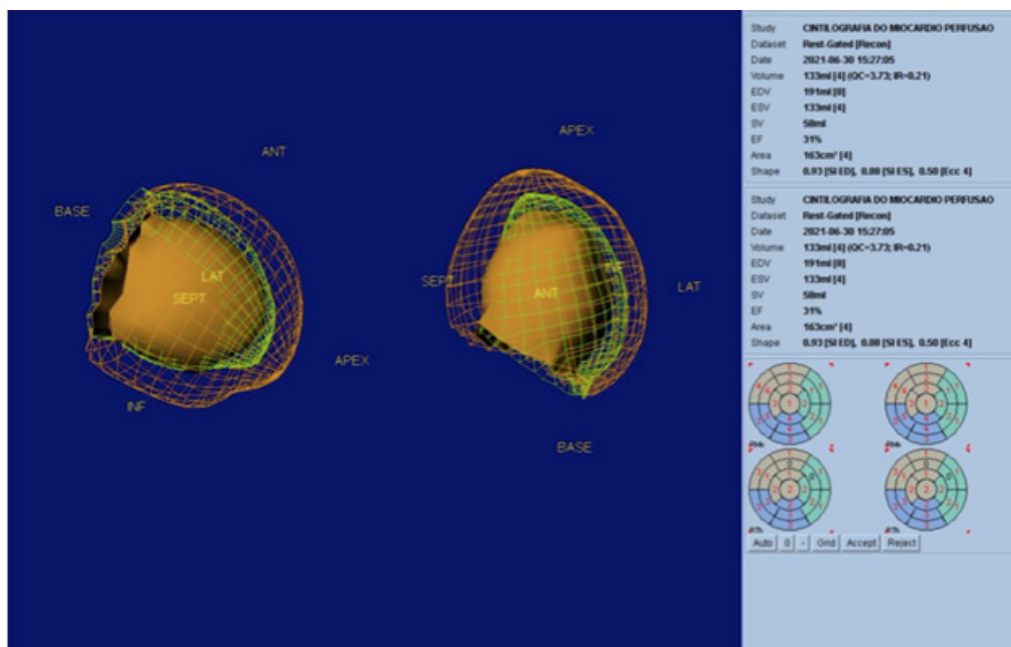


**Figure 6** – Gated-SPECT em repouso com uma reconstrução tridimensional do ventrículo esquerdo demonstrando fração de ejeção de 31%, aumento dos volumes ventriculares, acinesia inferior e discinesia inferosseptal. SPECT: tomografia computadorizada de emissão de fóton único.

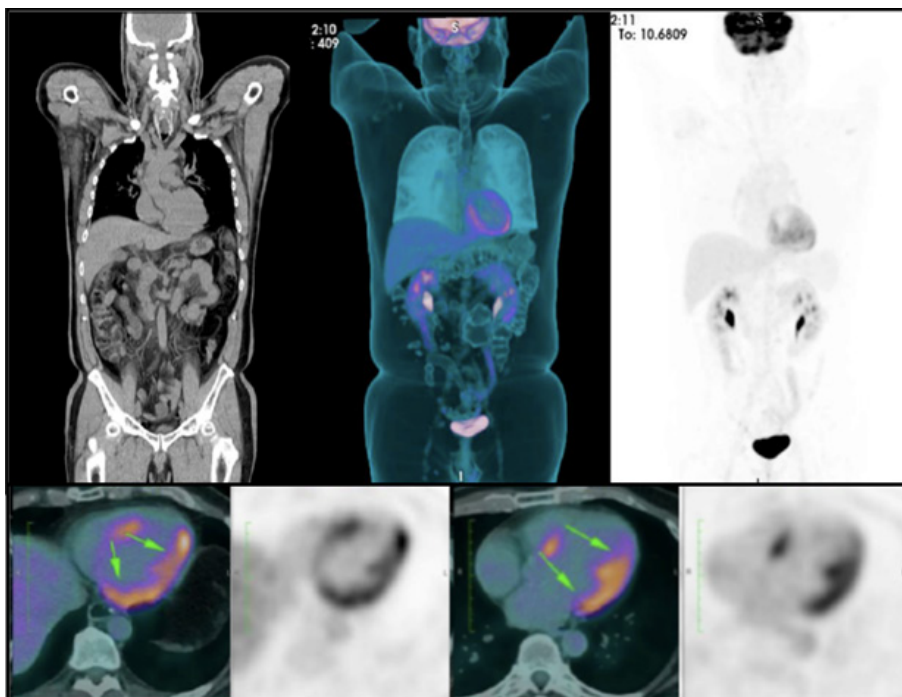


**Figura 7** – Resting gated-SPECT with three-dimensional reconstruction of the left ventricle demonstrating ejection fraction of 31%, increased ventricular volumes, inferior akinesia, and inferoseptal dyskinesia. SPECT: single-photon emission computed tomography.

### Use of Artificial Intelligence

The authors did not use any artificial intelligence tools in the development of this work.

### Availability of Research Data

The underlying content of the research text is contained within the manuscript.

## References

1. Mathai SV, Patel S, Jorde UP, Rochlani Y. Epidemiology, Pathogenesis, and Diagnosis of Cardiac Sarcoidosis. *Methodist Debakey Cardiovasc J*. 2022;18(2):78-93. doi: 10.14797/mdcvj.1057.
2. Birnie DH, Nery PB, Ha AC, Beanlands RS. Cardiac Sarcoidosis. *J Am Coll Cardiol*. 2016;68(4):411-21. doi: 10.1016/j.jacc.2016.03.605.
3. Cheng RK, Kittleson MM, Beavers CJ, Birnie DH, Blankstein R, Bravo PE, et al. Diagnosis and Management of Cardiac Sarcoidosis: A Scientific Statement from the American Heart Association. *Circulation*. 2024;149(21):e1197-e1216. doi: 10.1161/CIR.0000000000001240.
4. Sharma A, Okada DR, Yacoub H, Chrispin J, Bokhari S. Diagnosis of Cardiac Sarcoidosis: An Era of Paradigm Shift. *Ann Nucl Med*. 2020;34(2):87-93. doi: 10.1007/s12149-019-01431-z.
5. Birnie DH, Sauer WH, Bogun F, Cooper JM, Culver DA, Duvernoy CS, et al. HRS Expert Consensus Statement on the Diagnosis and Management of Arrhythmias Associated with Cardiac Sarcoidosis. *Heart Rhythm*. 2014;11(7):1305-23. doi: 10.1016/j.hrthm.2014.03.043.
6. Terasaki F, Azuma A, Anzai T, Ishizaka N, Ishida Y, Isobe M, et al. JCS 2016 Guideline on Diagnosis and Treatment of Cardiac Sarcoidosis—Digest Version. *Circ J*. 2019;83(11):2329-88. doi: 10.1253/circj.CJ-19-0508.
7. Agrawal T, Saleh Y, Sukkari MH, Alnabelsi TS, Khan M, Kassi M, et al. Diagnosis of Cardiac Sarcoidosis: A Primer for Non-Imagers. *Heart Fail Rev*. 2022;27(4):1223-33. doi: 10.1007/s10741-021-10126-5.
8. Terasaki F, Yoshinaga K. New Guidelines for the Diagnosis of Cardiac Sarcoidosis in Japan. *Ann Nucl Cardiol*. 2017;3(1):42-5.
9. Murtagh G, Laffin LJ, Patel KV, Patel AV, Bonham CA, Yu Z, et al. Improved Detection of Myocardial Damage in Sarcoidosis Using Longitudinal Strain in Patients with Preserved Left Ventricular Ejection Fraction. *Echocardiography*. 2016;33(9):1344-52. doi: 10.1111/echo.13281.
10. Slart RHJA, Claudemans AWJM, Gheysens O, Lubberink M, Kero T, Dweck MR, et al. Procedural Recommendations of Cardiac PET/CT Imaging: Standardization in Inflammatory-, Infective-, Infiltrative-, and Innervation (4Is)-Related Cardiovascular Diseases: A Joint Collaboration of the EACVI and the EANM. *Eur J Nucl Med Mol Imaging*. 2021;48(4):1016-39. doi: 10.1007/s00259-020-05066-5.
11. Aitken M, Chan MV, Fresno CU, Farrell A, Islam N, McInnes MDF, et al. Diagnostic Accuracy of Cardiac MRI versus FDG PET for Cardiac Sarcoidosis: A Systematic Review and Meta-Analysis. *Radiology*. 2022;304(3):566-79. doi: 10.1148/radiol.213170.
12. Stevenson A, Bray JJH, Tregidgo L, Ahmad M, Sharma A, Ng A, et al. Prognostic Value of Late Gadolinium Enhancement Detected on Cardiac Magnetic Resonance in Cardiac Sarcoidosis. *JACC Cardiovasc Imaging*. 2023;16(3):345-57. doi: 10.1016/j.jcmg.2022.10.018.
13. Okasha O, Kazmirczak F, Chen KA, Farzaneh-Far A, Shenoy C. Myocardial Involvement in Patients with Histologically Diagnosed Cardiac Sarcoidosis: A Systematic Review and Meta-Analysis of Gross Pathological Images from Autopsy or Cardiac Transplantation Cases. *J Am Heart Assoc*. 2019;8(10):e011253. doi: 10.1161/JAHA.118.011253.
14. Chareonthaitawee P, Beanlands RS, Chen W, Dorbala S, Miller EJ, Murthy VL, et al. Joint SNMMI-ASNC Expert Consensus Document on the Role of 18F-FDG PET/CT in Cardiac Sarcoid Detection and Therapy Monitoring. *J Nucl Cardiol*. 2017;24(5):1741-58. doi: 10.1007/s12350-017-0978-9.
15. Aitken M, Davidson M, Chan MV, Fresno CU, Vasquez LI, Huo YR, et al. Prognostic Value of Cardiac MRI and FDG PET in Cardiac Sarcoidosis: A Systematic Review and Meta-Analysis. *Radiology*. 2023;307(2):e222483. doi: 10.1148/radiol.222483.
16. Kumita S, Yoshinaga K, Miyagawa M, Momose M, Kiso K, Kasai T, et al. Recommendations for 18F-Fluorodeoxyglucose Positron Emission Tomography Imaging for Diagnosis of Cardiac Sarcoidosis-2018 Update: Japanese Society of Nuclear Cardiology Recommendations. *J Nucl Cardiol*. 2019;26(4):1414-33. doi: 10.1007/s12350-019-01755-3.
17. Lee PI, Cheng G, Alavi A. The Role of Serial FDG PET for Assessing Therapeutic Response in Patients with Cardiac Sarcoidosis. *J Nucl Cardiol*. 2017;24(1):19-28. doi: 10.1007/s12350-016-0682-1.
18. Trivieri MC, Robson PM, Vergani V, LaRocca C, Romero-Daza AM, Abgral R, et al. Hybrid Magnetic Resonance Positron Emission Tomography is Associated with Cardiac-Related Outcomes in Cardiac Sarcoidosis. *JACC Cardiovasc Imaging*. 2024;17(4):411-24. doi: 10.1016/j.jcmg.2023.11.010.
19. Greulich S, Gatidis S, Gräni C, Blankstein R, Glatthaar A, Mezger K, et al. Hybrid Cardiac Magnetic Resonance/Fluorodeoxyglucose Positron Emission Tomography to Differentiate Active from Chronic Cardiac Sarcoidosis. *JACC Cardiovasc Imaging*. 2022;15(3):445-56. doi: 10.1016/j.jcmg.2021.08.018.



This is an open-access article distributed under the terms of the Creative Commons Attribution License